Hydrogen-bond-directed supramolecular arrays in 4,4′-bipyridinium tetrachloroterephthalate dihydrate and bis(1,10-phenanthrolinium) tetrachloroterephthalate tetrachloroterephthalic acid trihydrate

Ming-Yang He,[a,b]* Zhi-Hui Zhang,[b] Lu-De Lu,[a] Xu-Jie Yang[a] and Xin Wang[a]

[a]School of Chemistry and Chemical Engineering, Nanjing University of Science and Technology, Nanjing 210093, People's Republic of China, and [b]Key Laboratory of Fine Petro-chemical Technology, Jiangsu Polytechnic University, Changzhou 213164, People's Republic of China

Correspondence e-mail: hemingyangjpu@yahoo.com

The title compounds, $C_{10}H_{10}N_2^{2+} \cdot C_8Cl_4O_4^{2-} \cdot 2H_2O$, (I), and $2C_{12}H_9N_2^+ \cdot C_8Cl_4O_4^{2-} \cdot C_8H_2Cl_4O_4 \cdot 3H_2O$, (II), both crystallize as charge-transfer organic salts with the dianionic or neutral acid components lying on inversion centres. The acid and base subunits in (I) arrange alternately to generate a linear tape motif via N—H···O hydrogen bonds; these tapes are further combined into a three-dimensional architecture through multiple O—H···O and C—H···O interactions involving solvent water molecules. In contrast, the neutral and anionic acid components in (II) are linked to form a zigzag chain by means of O—H···O hydrogen bonds between acid groups, with dangling 1,10-phenanthrolinium units connected to these chains by carboxylate–pyridinium interactions with $R_2^2(7)$ hydrogen-bond notation. Adjacent chains are further extended to result in a two-dimensional corrugated layer network via π–π interactions. Inter-ion Cl···O interactions are also found in both (I) and (II).

Comment

The supramolecular synthon approach has been widely applied to tailor desired supramolecules and molecular solids by using previously identified robust intermolecular interactions since it offers a considerable simplification in the design of crystal structures (Desiraju, 1995; Nangia & Desiraju, 1998). For the cocrystal structures of carboxylic acids with pyridyl building blocks, strong hydrogen bonds, such as O—H···N or charge-assisted N—H···O, are always essential, usually combined with auxiliary weak C—H···O interactions, leading to the most familiar carboxyl/pyridyl heterosynthon

[graph set $R_2^2(7)$; Etter, 1990; Shan et al., 2002]. In this context, although aromatic dicarboxylic acids have proved to be excellent building blocks in binary cocrystal assemblies with bipyridine-type components, terephthalic acid (H_2tp) has been less well studied than phthalic acid and isophthalic acid in this respect owing to the mismatched solubility with base components, especially because of the poor solubility of H_2tp (Du et al., 2005). Related efforts on its derivatives have been rare so far. Notably, it can be forecast that the substituent groups will influence the structural assemblies, since they may display different hydrogen-bonding capability and potential steric/electronic effects. A search of the Cambridge Structural Database (CSD; Version 5.30 of November 2008, plus two updates; Allen, 2002) reveals that no organic structure based on a halogen functional terephthalic acid has been reported to date, except for a supramolecular adduct of triethylammonium with tetrachloroterephthalic acid (H_2tpCl$_4$; Lan et al., 2008). In this present work, two charge-transfer crystalline products, that is (H_2bipy)(tpCl$_4$)·2H_2O (bipy is 4,4′-bipyridine), (I), and (Hphen)$_2$(H_2tpCl$_4$)(tpCl$_4$)·3H_2O (phen is 1,10-phenanthroline), (II), were prepared.
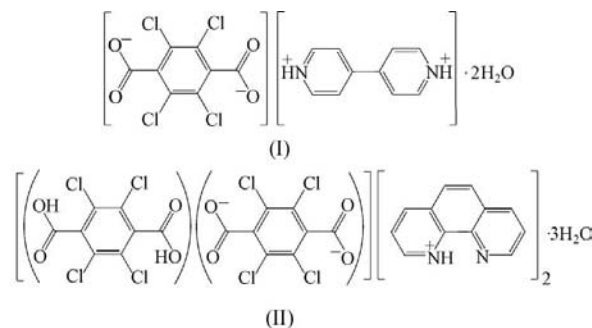
Compound (I) is shown to be a proton-transfer organic binary salt, in which the asymmetric unit is composed of half of a tpCl$_4^{2-}$ anion, half of an H_2bipy^{2+} cation (both lying about independent inversion centres) and one solvent water molecule in a general position (Fig. 1). Proton transfer from the tetrachloroterephthalic acid to the 4,4′-bipyridine moiety was unequivocally established from difference map plots, and the resulting cation and anion dimensions are normal and fully in accord with this proton-transfer scheme. Because the two pyridinium rings are related by an inversion centre, the
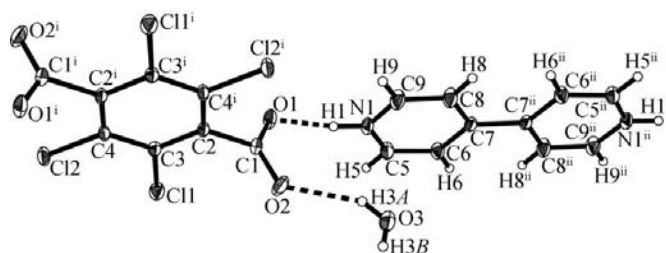

Figure 1
The molecular structure of (I), drawn with 30% probability displacement ellipsoids. Hydrogen bonds are indicated by dashed lines. [Symmetry codes: (i) −x + 2, −y + 1, −z + 1; (ii) −x, −y + 2, −z + 2.]
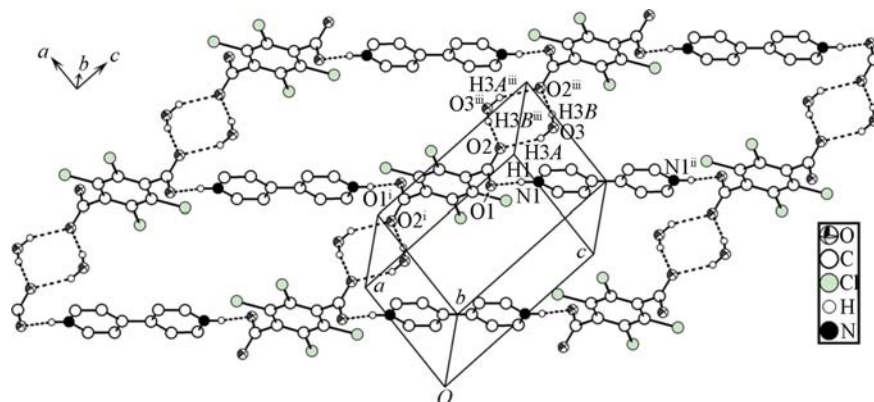
Figure 2
The two-dimensional hydrogen-bonded layer of (I). Hydrogen bonds are indicated by dashed lines. [Symmetry codes: (i) $-x + 2, -y + 1, -z + 1$; (ii) $-x, -y + 2, -z + 2$; (iii) $-x + 2, -y + 1, -z + 2$.]

dihedral angle between them is exactly 0°. In the centrosymmetric tpCl₄²⁻ ion, the unique carboxylate group is nearly perpendicular [87.4 (2)°] to the aromatic ring, as influenced by the stereo-hindrance of the adjacent chloro substituents. The plane of the aromatic ring of the tpCl₄²⁻ anion is inclined at 3.96 (9)° to that of the bipy component.

In the crystal structure of (I) (Fig. 2), linear tapes are generated through strong N1—H1···O1 hydrogen bonds (Table 1) between carboxylate and pyridinium groups; these tapes run along the crystallographic [2$\overline{1}\overline{1}$] direction with a graph-set motif of $C_2^2(18)$ (Etter, 1990). Notably, the anticipated $R_2^2(7)$ synthon of N—H···O/C—H···O is absent owing to the approximately perpendicular dihedral angle [83.52 (13)°] between the carboxylate and pyridinium groups. The solvent water molecule is involved in two strong hydrogen bonds (O3—H3A···O2 and O3—H3B···O2ⁱⁱⁱ; symmetry codes and geometric parameters are given in Table 1) with carboxylate atom O2 of tpCl₄²⁻, which leads to an eight-membered hydrogen-bonded $R_4^2(8)$ ring and gives rise to a linear (tpCl₄²⁻·2H₂O)ₙ chain extending along the c-axis direction. Such hydrogen-bonding interactions connect neighboring tapes, resulting in a two-dimensional layer, as shown in Fig. 2. These layers align parallel to the (120) plane with some offset to fulfil the final three-dimensional hydrogen-bonding framework, which is generated via weak C—H···O interactions (C6—H6···O3ⁱᵛ and C8—H8···O3ᵛ; Table 1) between bipyridinium cations and water molecules from adjacent layers. Additionally, intermolecular C4—Cl2···O3ᵛⁱ [symmetry code: (vi) $x + 1, y, z - 1$] interactions link water molecules to further consolidate the three-dimensional assembly, with a Cl···O distance of 3.040 (2) Å, modestly shorter than the van der Waals distance (3.12 Å) suggested by Nyburg & Faerman (1985).

Crystallization of tetrachloroterephthalic acid with phenanthroline also yields a proton-transfer organic salt, (II). The crystal structure of (II) exhibits a two-dimensional supramolecular host network with the inclusion of disordered guest water molecules (Fig. 3). The asymmetric unit is composed of half of an H₂tpCl₄ molecule and half of a tpCl₄²⁻ anion (both

lying about independent inversion centres), one monoprotonated Hphen⁺ cation in a general position and 1.5 disordered guest water molecules lying about another inversion centre. Proton transfer from a tetrachloroterephthalic acid molecule to the phen molecule was unequivocally established from difference map plots, and the resulting cation and anion dimensions are normal and fully in accord with this proton-transfer scheme.

As shown in Fig. 3, within each centrosymmetric acidic unit, the dihedral angles between the carboxylate/carboxyl groups and those of the tetrachlorinated aromatic rings are 77.8 (2)° for tpCl₄²⁻ and 89.9 (1)° for H₂tpCl₄. The dihedral angle in the dianion is smaller than the corresponding values for other polychlorinated carboxylate compounds [80.6 (4) and 89.7 (3)° (Maspoch *et al.*, 2004), and 81.88 (13)–90.0 (1)° (Chen *et al.*, 2008)]. Analysis of the crystal packing of (II) shows that the neutral and dianionic acid moieties are connected by intermolecular O1—H1′···O3 hydrogen bonds to form a one-dimensional zigzag chain structure extending in the (101) direction (Fig. 4). Meanwhile, each tpCl₄²⁻ dianion is linked to monoprotonated Hphen⁺ cations with an $R_2^2(7)$ ring pattern via N1—H1A···O3 and C10—H10···O4 hydrogen bonds (Table 2). Adjacent inversion-related Hphen⁺ ions take part in π–π interactions; the centroid (Cg1) of the N1/C7–C10/C12 ring is 3.556 (2) Å from the centroid (Cg2) of the C4–C7/C11/C12 ring at $(-x + 1, -y + 2, -z + 1)$; this also allows a further C6—H6···O2ⁱᵛ (Table 2) interaction and expands the one-dimensional zigzag motif into a two-dimensional hydrogen-bonding network (Fig. 5). The disordered solvent water subunits are captured in the two-dimensional supramolecular layer with partial-occupancy water atom O52 lying
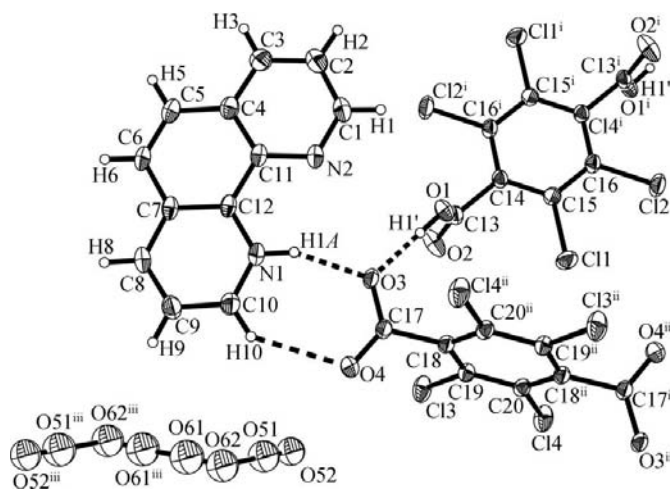

Figure 3
The molecular structure of (II), drawn with 30% probability displacement ellipsoids. Hydrogen bonds are indicated by dashed lines. [Symmetry codes: (i) $-x + 2, -y + 1, -z + 1$; (ii) $-x + 1, -y + 1, -z$; (iii) $-x, -y + 2, -z$.]

2.765 (7) Å from adjacent carboxylate atom O4. Adjoining two-dimensional layers are further extended to a three-dimensional arrangement through intermolecular C20—Cl4⋯O4^v [Cl⋯O = 3.265 (2) Å and C—Cl⋯O = 144.42 (10)°; symmetry code: (v) $x + 1$, y, z] interactions.

In conclusion, this work demonstrates the first example of H$_2$tpCl$_4$ as a good participant in cocrystallization with aromatic diamines. When cocrystallizing with the rod-like 4,4′-bipyridine building block, the H$_2$tpCl$_4$ subunits reliably form N—H⋯O interactions, while in the case of 2,2′-bipyridine-type moieties, only one of the phenanthroline N-atom donors forms an $R_2^2(7)$ heterosynthon with anionic tpCl$_4$ as a result of the stereochemistry effect of the phen molecule. Both the acid–base adducts show organic binary salts behaving as charge-assisted hydrogen-bonding structures of considerable multiplicity. This result offers a new challenge in the search for true neutral cocrystals based on such halogen-substituted terephthalic acids.
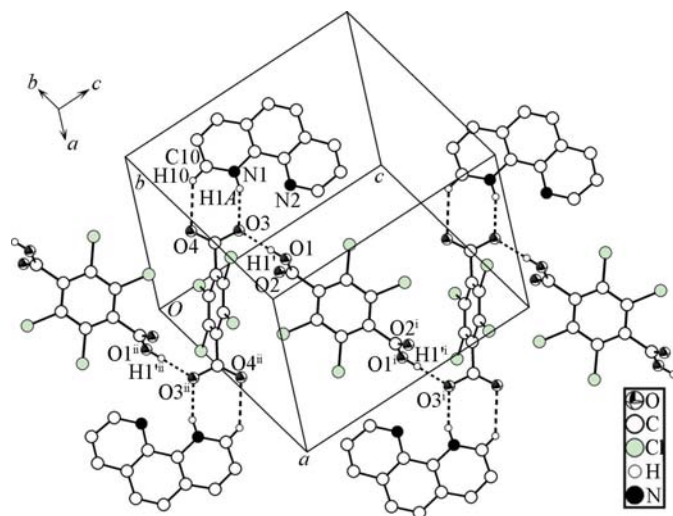

Figure 4
A partial view of the one-dimensional zigzag motif of (II). Hydrogen bonds are indicated by dashed lines. [Symmetry codes: (i) $-x + 2$, $-y + 1$, $-z + 1$; (ii) $-x + 1$, $-y + 1$, $-z$.]
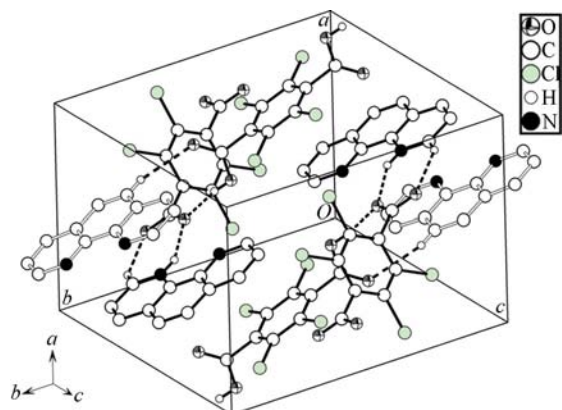

Figure 5
The two-dimensional hydrogen-bonded layer of (II), with hydrogen bonds indicated by dashed lines. The disordered water guests within the cavities have been omitted for clarity.

Experimental

Compound (I)

Crystal data

C$_{10}$H$_{10}$N$_2$$^{2+}$·C$_8Cl_4O_4$$^{2-}$·2H$_2$O	γ = 73.842 (4)°
M_r = 496.11	V = 501.3 (3) Å^3
Triclinic, $P\bar{1}$	Z = 1
a = 6.306 (2) Å	Mo $K\alpha$ radiation
b = 9.325 (3) Å	μ = 0.63 mm^{-1}
c = 10.040 (4) Å	T = 296 K
α = 62.508 (3)°	0.18 × 0.15 × 0.12 mm
β = 86.763 (4)°	

Data collection

Bruker APEXII CCD area-detector diffractometer	3529 measured reflections
	1732 independent reflections
Absorption correction: multi-scan (*SADABS*; Sheldrick, 2003)	1590 reflections with $I > 2\sigma(I)$
T_{min} = 0.895, T_{max} = 0.928	R_{int} = 0.033

Refinement

$R[F^2 > 2\sigma(F^2)]$ = 0.039	136 parameters
$wR(F^2)$ = 0.128	H-atom parameters constrained
S = 1.00	$\Delta\rho_{max}$ = 0.40 e Å^{-3}
1732 reflections	$\Delta\rho_{min}$ = −0.47 e Å^{-3}

Table 1
Hydrogen-bond geometry (Å, °) for (I).

D—H⋯A	D—H	H⋯A	D⋯A	D—H⋯A
N1—H1⋯O1	0.90	1.72	2.609 (3)	169
O3—H3A⋯O2	0.82	2.08	2.824 (3)	151
O3—H3B⋯O2^{iii}	0.82	1.98	2.778 (3)	165
C6—H6⋯O3^{iv}	0.93	2.35	3.269 (4)	169
C8—H8⋯O3^v	0.93	2.57	3.492 (4)	172

Symmetry codes: (iii) $-x + 2$, $-y + 1$, $-z + 2$; (iv) $-x + 1$, $-y + 2$, $-z + 2$; (v) $x - 1$, y, z.

Compound (II)

Crystal data

2C$_{12}$H$_9$N$_2$$^+$·C$_8Cl_4O_4$$^{2-}$··C$_8H_2Cl_4O_4$·3H$_2$O	β = 109.454 (1)°
	γ = 106.072 (2)°
M_r = 1022.25	V = 1054.4 (2) Å^3
Triclinic, $P\bar{1}$	Z = 1
a = 8.2931 (11) Å	Mo $K\alpha$ radiation
b = 12.0916 (16) Å	μ = 0.60 mm^{-1}
c = 12.3108 (16) Å	T = 295 K
α = 102.127 (2)°	0.28 × 0.22 × 0.15 mm

organic compounds

Bruker APEXII CCD area-detector diffractometer
Absorption correction: multi-scan (*SADABS*; Sheldrick, 2003) $T_{min} = 0.850$, $T_{max} = 0.915$

7609 measured reflections
3677 independent reflections
3201 reflections with $I > 2\sigma(I)$
$R_{int} = 0.020$

Refinement

$R[F^2 > 2\sigma(F^2)] = 0.044$
$wR(F^2) = 0.147$
$S = 1.07$
3677 reflections

288 parameters
H-atom parameters constrained
$\Delta\rho_{max} = 0.73$ e Å^{-3}
$\Delta\rho_{min} = -0.38$ e Å^{-3}

Table 2
Hydrogen-bond geometry (Å, °) for (II).

$D-H\cdots A$	$D-H$	$H\cdots A$	$D\cdots A$	$D-H\cdots A$
O1—H1′···O3	0.82	1.74	2.550 (3)	170
N1—H1A···O3	0.90	1.95	2.788 (4)	154
C6—H6···O2^{iv}	0.93	2.56	3.413 (5)	152
C10—H10···O4	0.93	2.43	3.193 (4)	139

Symmetry code: (iv) $-x+1, -y+2, -z+1$.

H atoms bonded to C atoms were positioned geometrically (C—H = 0.93 Å) and included in the refinement in the riding-model approximation, with $U_{iso}(H)$ values set at $1.2U_{eq}(C)$. In (II), the electron-density maps showed that water molecule O5 is disordered unequally over two sites, consistent with occupancies of 0.6 and 0.4; water molecule O6 has electron density consistent with it being a one-quarter occupancy O atom disordered equally over two pairs of sites sitting about a centre of inversion. It was not possible to locate any of these water H atoms. All of the other water and amine H atoms were initially located in difference maps, then geometrically optimized and refined as riding, with $U_{iso}(H)$ values of $1.5U_{eq}(O,N)$.

For both compounds, data collection: *APEX2* (Bruker, 2007); cell refinement: *APEX2* and *SAINT* (Bruker, 2007); data reduction: *SAINT*; program(s) used to solve structure: *SHELXTL* (Sheldrick, 2008); program(s) used to refine structure: *SHELXTL*; molecular graphics: *SHELXTL* and *DIAMOND* (Brandenburg, 2005); software used to prepare material for publication: *SHELXTL*.

References

Allen, F. H. (2002). *Acta Cryst.* B**58**, 380–388.
Brandenburg, K. (2005). *DIAMOND*. Version 3.0d. Crystal Impact GbR, Bonn, Germany.
Bruker (2007). *APEX2* and *SAINT*. Bruker AXS Inc., Madison, Wisconsin, USA.
Chen, Q., Xie, Y., Li, C., He, M. & Chen, S. (2007). *Acta Cryst.* E**63**, o4549.
Chen, S.-C., Zhang, Z.-H., Huang, K.-L., Chen, Q., He, M.-Y., Cui, A.-J., Li, C., Liu, Q. & Du, M. (2008). *Cryst. Growth Des.* **8**, 3437–3445.
Desiraju, G. R. (1995). *Angew. Chem. Int. Ed. Engl.* **34**, 2311–2327.
Du, M., Zhang, Z.-H. & Zhao, X.-J. (2005). *Cryst. Growth Des.* **5**, 1199–1208.
Etter, M. C. (1990). *Acc. Chem. Res.* **23**, 120–126.
Lan, F.-F., Xu, X.-B., Yang, S.-Y. & Huang, R.-B. (2008). *J. Chem. Crystallogr.* **38**, 743–747.
Maspoch, D., Domingo, N., Ruiz-Molina, D., Wurst, K., Tejada, J., Rovira, C. & Veciana, J. (2004). *J. Am. Chem. Soc.* **126**, 730–731.
Nangia, A. & Desiraju, G. R. (1998). *Acta Cryst.* A**54**, 934–944.
Nyburg, S. C. & Faerman, C. H. (1985). *Acta Cryst.* B**41**, 274–279.
Shan, N., Bond, A. D. & Jones, W. (2002). *Cryst. Eng.* **5**, 9–24.
Sheldrick, G. M. (2003). *SADABS*. Version 2.10. University of Göttingen, Germany.
Sheldrick, G. M. (2008). *Acta Cryst.* A**64**, 112–122.

o528 He *et al.* · $C_{10}H_{10}N_2^{2+}\cdot C_8Cl_4O_4^{2-}\cdot 2H_2O$ and $2C_{12}H_9N_2^+\cdot C_8Cl_4O_4^{2-}\cdot C_8H_2Cl_4O_4\cdot 3H_2O$

Acta Cryst. (2009). C**65**, o525–o528